

Research Article

Analysis of the Multiwalled Carbon Nanotubes Reinforced Polymethyl Methacrylate Bone Cement's Characteristics and *In Vitro* Bioactivity to Prolong Its Functionality in Orthopedic Application

T. V. Vineeth Kumar ¹, N. Shanmugapriya ¹, S. Arun ², and G. Ramasubramanian ³

¹Department of Mechanical Engineering, Siddaganga Institute of Technology (Autonomous Institution Affiliated to Visvesvaraya Technological University, Belagavi), Tumakuru, 572 103 Karnataka, India

²Advanced Composites Division, CSIR-National Aerospace Laboratories, Bengaluru, 560 017 Karnataka, India

³Department of Chemistry, Seenu Atoll School, Addu City, Maldives

Correspondence should be addressed to G. Ramasubramanian; raman@satollschoo.edu.mv

Received 24 December 2022; Revised 23 March 2023; Accepted 27 April 2023; Published 30 May 2023

Academic Editor: Indran Suyambulingam

Copyright © 2023 T. V. Vineeth Kumar et al. This is an open access article distributed under the Creative Commons Attribution License, which permits unrestricted use, distribution, and reproduction in any medium, provided the original work is properly cited.

Polymethyl methacrylate (PMMA) bone cement is being used to fill voids that are created due to vertebral compression fractures. It is also a grouting medium in orthopedic joint replacement surgeries as they possess fast primary fixation to the bone. Considering the cement properties and *in vitro* bioactivity of bone cement is essential for cemented hip and knee joint replacement surgeries. In this study, commercial Simplex P bone cement (SPBC) is modified with carboxyl- (-COOH-) functionalized multiwalled carbon nanotubes (MWCNTs) to overcome high polymerization temperature, volumetric shrinkage, surface wettability, and *in vitro* bioactivity. A geometric dilution method is used to incorporate MWCNTs with the PMMA powder, which is in unequal proportions. The PMMA/MWCNT nanocomposite with different concentrations of reinforcements, such as 0.1, 0.3, 0.5, and 0.7 weight percentages, is prepared for the investigation. It was observed that the MWCNTs had a beneficial impact on PMMA bone cement (PMMA-BC) by enhancing its setting time (2.94%↑) and surface wettability (23.58%↑). Also, diminished polymerization temperature (29%↓) and volumetric shrinkage (40.9%↓) are observed for an optimum concentration of 0.7 wt. %. The bioactivity of the cement surface is validated by the *in vitro* bioactivity observed in simulated body fluid (SBF) through the development of primary and secondary apatite. It is concluded that the synthesized PMMA/MWCNT nanocomposites are found to have enhanced cement properties compared to PMMA-BC.

1. Introduction

PMMA bone cement has been used to secure prosthetic joints in humans for over fifty years [1]. The PMMA is a self-polymerizing polymer that allows for a fast primary fixation to the bone and helps in speedy patient recovery after surgery. Also, it is simple to handle during the preparation and positioning of cement mantles [2]. This self-setting PMMA bone cement fills the gap and distributes the load between the bone and implant in hip and knee joint replacement surgeries [3]. The compression fracture voids were

filled by the percutaneous injection of PMMA-BC into the vertebral body [4]. The PMMA was observed to lose its properties after its prolonged usage, which leads to revision surgery. The prominent reasons for the failure of cemented joint replacements are aseptic loosening, volumetric shrinkage, and breakdown of the cement mantle [5, 6]. PMMA-BC undergoes a high exothermic polymerization reaction that generates temperatures beyond 100°C. These high polymerization temperatures can result in significant thermal necrosis and aseptic loosening [7]. According to reports, bone tissue experiences thermal necrosis after being exposed to

temperatures beyond 50°C for more than one minute. It has been revealed that the reasons for volumetric shrinkage are thermal contraction (upon cooling) and variation in density during polymerization [8]. Gilbert et al. [9] reported 5.1% to 6.5% volumetric shrinkage as a result of density change brought on by exothermic polymerization. Thus, the technical issues with the current use of bone cement are listed as high polymerization temperature causing thermal necrosis, excessive volumetric shrinkage leading to mechanical loosening, and short working times causing uneven filling [10].

The aforesaid shortcomings of PMMA bone cement attracted researchers to work on bone cement properties by incorporating different fillers like graphene oxide, silver nanoparticles, silica nanoparticles, carbon nanotubes, and other fillers [11–13]. It can be noted from the literature that nanomaterials have been used prominently as fillers because they differ from bulk materials of the same composition in terms of strong reactivity and the substantial surface area-to-mass ratio [14]. The properties of nanomaterials are intrinsic only if they are distributed uniformly in the matrix. The MWCNTs were reinforced with PMMA-BC to enhance the cement properties. The agglomeration of MWCNTs within the bone cement matrix is governed mainly by the method used to distribute them into the bone cement matrix [15]. The distribution of MWCNTs in the bone cement matrix was achieved by the following three methods [16]:

- (1) *Ultrasonic Disintegrator*. MWCNTs were incorporated into liquid monomer by dispersion
- (2) *High-Temperature Mechanical Shear Mixing*. MWCNTs were dispersed with MMA powder
- (3) *Magnetic Stirring*. MWCNTs were incorporated into liquid monomers using a magnetic stirrer

The thermal properties obtained by Ormsby et al. [16] for 0.1 wt.% unfunctionalized and -COOH-functionalized MWCNT-reinforced bone cement using the above three methods are summarized in Table 1. The amount of heat released during the exothermic polymerization of PMMA-BC was greatly influenced by the addition of functionalized MWCNTs.

The literature review indicates that MWCNTs were dispersed in the liquid component of the bone cement using sonication and magnetic-stirring methods. MWCNTs were added to the MMA powder component in the dry blending technique. However, these methods required additionally a sophisticated instrument and postprocessing methods for the incorporation of MWCNTs. Although the results were encouraging, it is a difficult task to significantly improve the overall performance of the nanocomposites without compromising mechanical and physical properties. The scientific community is still grappling with the issues of PMMA-BC processing methods for uniform disaggregation and poor chemical interface with the matrix [17].

In this study, MWCNTs are incorporated into the powder part of PMMA-BC using a geometric dilution method, which is often used in the pharmaceutical industry to mix two powders of unequal proportions [18]. This method is

used as an alternative to sonication and magnetic stirring methods to incorporate MWCNTs to reduce possible agglomeration. The effect of 0.1, 0.3, 0.5, and 0.7 wt. % MWCNT-COOH on commercial SPBC in terms of cement properties and *in vitro* bioactivity is reported in this work. Fourier transform infrared (FTIR) was used to investigate the chemical interaction (identification of compounds) with the PMMA-BC matrix. The physical interface of MWCNTs with PMMA is detected using Transmission electron microscopy (TEM).

2. Materials and Methods

2.1. Materials. The surgical Simplex P radiopaque bone cement is purchased from Stryker Howmedica Osteonics, Republic of Ireland. It is a two-part acrylic-based mixture with liquid and powder components. The powder component contains polymethyl methacrylate polymer units, barium sulfate as a radiopaque agent, and benzoyl peroxide as the polymerization initiator. The composite composition uses carboxyl functionalized MWCNTs as nanofillers, purchased from Platonic Nanotech Pvt. Ltd. (Kachwa Chowk, Mahagama, Jharkhand) that are 2–10 μm in length and 10–15 nm in outer diameter.

2.2. Formulation of Composite Bone Cement. According to manufacturer recommendations, the powder and liquid medium are combined in a 2 : 1 ratio, initiating the polymerization of free radicals to form a rigid polymer. In Table 2, the weight ratios of the composite bone cement are displayed. Briefly, MWCNTs were dispersed using a geometrical dilution method with measured size, combining fine powders of unequal proportions of MWCNTs with MMA powder to ensure uniform distribution. This MMA powder and MWCNT blend are added to the MMA liquid monomer solution to initiate self-polymerization. Nanocomposite bone cement samples are prepared for 0.1, 0.3, 0.5, and 0.7 wt. % MWCNT concentration.

Mixing of liquid and powder components involves sticky, working, and hardening phases. The mixture is poured into the mould of 6 mm diameter and 12 mm height when it is seen to approach the dough stage. The curing is done at room temperature for 24 hours. The cylindrical specimens are cut into sections after curing and polished with SiC paper with grits ranging from 220 to 2400.

3. Thermal Characterization

3.1. Polymerization Temperature Measurements. The exothermic polymerization temperatures are measured for the nanocomposite bone cement samples using a digital infrared thermometer. The thermometer is calibrated at an ice point (0°C) and boiling point of water (100°C) for its precision. The temperatures are measured at 30 seconds intervals at the center and different locations of the cylindrical mould (ϕ6 × 12 mm), during the different stages of curing. The sample temperatures are recorded at different locations on the specimen to obtain a better estimation and the average of three maximum values are recorded.

TABLE 1: Thermal properties of PMMA-BC (Colacryl B866) with different methods of incorporation [16].

Methods of incorporation	Type of MWCNT	Maximum temperature % decrease	Setting time % increase
Ultrasonic disintegration	Unfunctionalized	9.57	51.87
	-COOH functionalized	8.05	55.90
Dry blending	Unfunctionalized	16.86	96.54
	-COOH functionalized	25.41	146.68
Magnetic stirring	Unfunctionalized	29.08	81.55
	-COOH functionalized	52.75	207.06

TABLE 2: Composite identification and composition.

Sl. No.	Sample identification	Material composition
1	BC	PMMA (control)
2	BC1	PMMA+0.1% MWCNT
3	BC2	PMMA+0.3% MWCNT
4	BC3	PMMA+0.5% MWCNT
5	BC4	PMMA+0.7% MWCNT

3.2. Setting Time. The prepared samples are tested for their setting time using a Vicat instrument. The initial and final setting times are measured by following the ASTM C191-08 standard [19]. The dial gauge measures the needle's vertical travel at a constant 100 g load. The needle is used to pierce a 10 × 50 mm bone cement mould. The tip's distance is measured at every 5 seconds until the cement gets cured.

3.3. Thermal Gravimetric Analysis. The thermal gravimetric analysis (TGA) of bone cement is investigated using differential scanning calorimetry (DSC)-TGA SDT2960 from ambient temperature to 700°C at 10°C/minute in nitrogen gas atmosphere. Before the DSC/TGA studies, the samples are hardened in a pH 7.4 phosphate-buffered saline solution. The samples are crushed, dried for 24 hours in the open air, and then tested.

4. Contact Angle

Contact angle measurements are used to quantify the surface wettability of the PMMA-BC samples. The static sessile drop method is employed to determine the contact angle using a fabricated contact angle measuring instrument. The contact angles are measured on five randomly chosen regions of each sample using distilled water droplets. As previously noted, samples of $\phi 10 \pm 2$ mm in size are made. Phosphate-buffered saline, which has a pH of 7.4, is used to harden the samples. SiC papers of 800 and 1200 grits are used to polish the bone cement samples to achieve a flat smooth surface. Before testing, the samples are dried for 24 hours after being sonicated for 30 min in an ultrasonic cleaner bath.

4.1. Volumetric Shrinkage. The volumetric shrinkage of the prepared nanocomposite bone cement is investigated after curing to observe the effect of MWCNTs on PMMA-BC volume change. The samples with different MWCNTs wt. % having a diameter of 6 mm and thickness of 12 mm are prepared and allowed to harden, as mentioned earlier.

The samples are dried for 24 hours, and the final volume is estimated as per ASTM D 792-20 by measuring densities using Archimedes' principle with a Mettler electronic balance—ME204. Standard specimen is used to calibrate the instrument. The density accuracy of ± 0.0001 g/cc is obtained using this method. The volumetric shrinkage is calculated using Equation (1),

$$\begin{aligned} \% \text{Volumetric Shrinkage} &= - \left(\frac{v_f - v_i}{v_i} \right) 100 \\ &= - \left(\frac{\rho_m - \rho_p}{\rho_p} \right) 100, \end{aligned} \quad (1)$$

where v_i is the initial volume (mL), v_f is the final volume (mL), ρ_m is the density of the monomer, (g/cc), and ρ_p is the density of the polymer (g/cc).

4.2. Fourier Transform Infrared Spectroscopy (FTIR). As previously stated, $\phi 10 \times 2$ mm samples are prepared for FTIR characterization. The samples are air dried for 24 hours before being powdered with an agate mortar and pestle. A Bruker Alpha II FTIR spectrophotometer is used to examine the functional groups of the pulverized composite. In transmission mode, spectra of the composite are observed in the spectral range of 4000–400 cm^{-1} to determine the chemical interactions between the MWCNTs and PMMA.

4.3. Electron Microscopy. The nanocomposite bone cement specimens are observed for morphology by using scanning electron microscopy (SEM) (JEOL 6500, JSM) at a working voltage of 5.0 kV and 4-Torr vacuum pressure. The prepared samples for SEM are dried for 24 hours and then polished using SiC paper (220–2400 grits), and they are sputter coated. Energy dispersive spectroscopy is used to investigate the elemental composition of the composite bone cement.

The powdered samples of nanocomposite bone cement are studied for morphology at the MWCNT-PMMA interphase using transmission electron microscopy (TEM)-HRTEM (JEOL/JEM 2100, Japan) having a point resolution of 0.23 nm operated at 120 kV.

4.4. In Vitro Bioactivity. The formation of apatite in the SBF has been used as an indication that an orthopedic material is bioactive. Samples ($n = 3$) of uniform size (8×2 mm) are examined for bioactivity by submerging them in SBF. Tris/HCl is added to set the pH of the solution as 7.4. The SBF-immersed samples are incubated at 37°C for a period of 7,

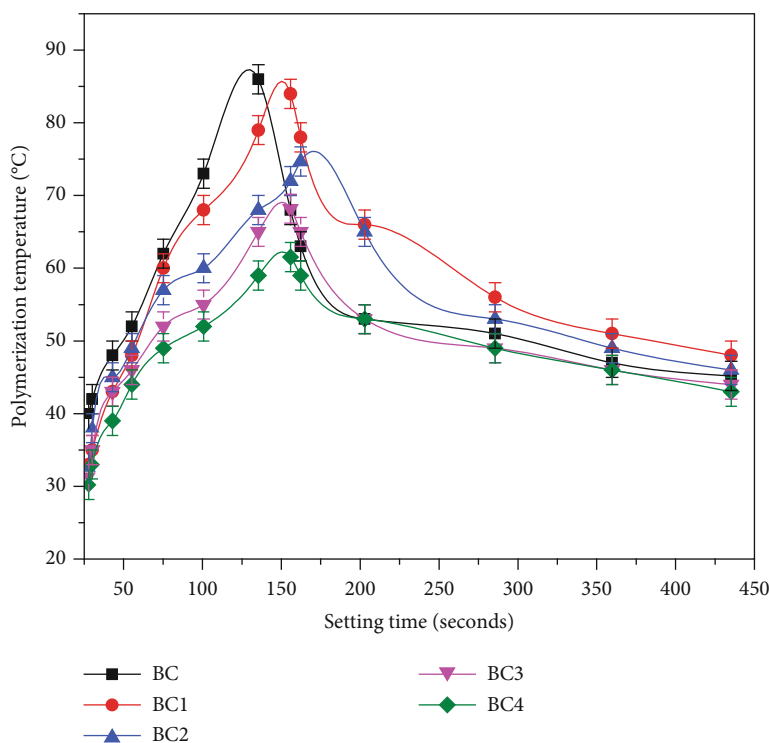


FIGURE 1: Setting time v/s polymerization temperatures.

14, and 21 days. After the designated incubation period, samples are rinsed with deionized water to eliminate adsorbed minerals and dried; then, SEM and EDS are analyzed for apatite deposition.

4.5. Statistical Analysis. The data for polymerization temperature, setting time, and contact angle are statistically analyzed using a two-sample *t*-test. To illustrate the results, the mean standard deviation is employed. The level of statistical significance is set at $p < 0.05$.

5. Results and Discussion

5.1. Thermal Characterization. The setting time concerning the polymerization temperature for different bone cement compositions is shown in Figure 1. The maximum polymerization temperature (T_{max}) is reduced for all compositions of the prepared composites. The maximum (84°C) and minimum (61°C) values of T_{max} are recorded for 0.1 and 0.7 wt. % of MWCNT loading, respectively. The temperature evolution of the PMMA-BC reached 86°C, whereas the inclusion of 0.7 wt.% MWCNTs reduced the peak polymerization temperature to 61°C in 160 seconds.

The variation of peak polymerization temperature (T_{max}) for different bone cement compositions with varying MWCNT loading is shown in Figure 2. The addition of 0.1, 0.3, 0.5, and 0.7 wt. % MWCNT to PMMA-BC resulted in a decrease of T_{max} . This decrease in T_{max} is influenced by the thermal conductivity of MWCNT, which is reported as 3000 W/mK [20]. Also, the MWCNTs within the PMMA matrix are observed to exhibit chemical interaction because of the -COOH func-

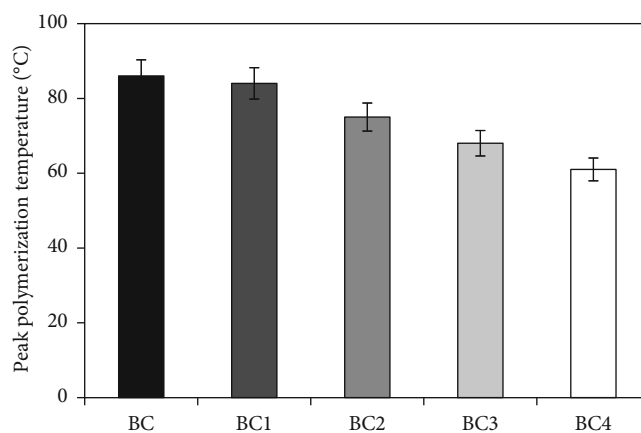


FIGURE 2: Variation in the peak polymerization temperature of composite bone cement.

tional group and physical interaction due to the large surface area during the polymerization reaction [15]. These interactions helped to dissipate the heat energy produced during polymerization.

TEM analysis is carried out to explore PMMA-MWCNT physical interaction and morphology of the nanocomposite particles. The TEM pictures, Figure 3(a) and 3(b), of the 0.7 wt. % MWCNT-loaded composite bone cement powder show that the agglomerated particles are observed as in the shape of beads and are about 75 nm in size. The TEM pictures also show the well-dispersed MWCNTs surrounded by PMMA particles, which ensures the physical interphase between PMMA-MWCNT.

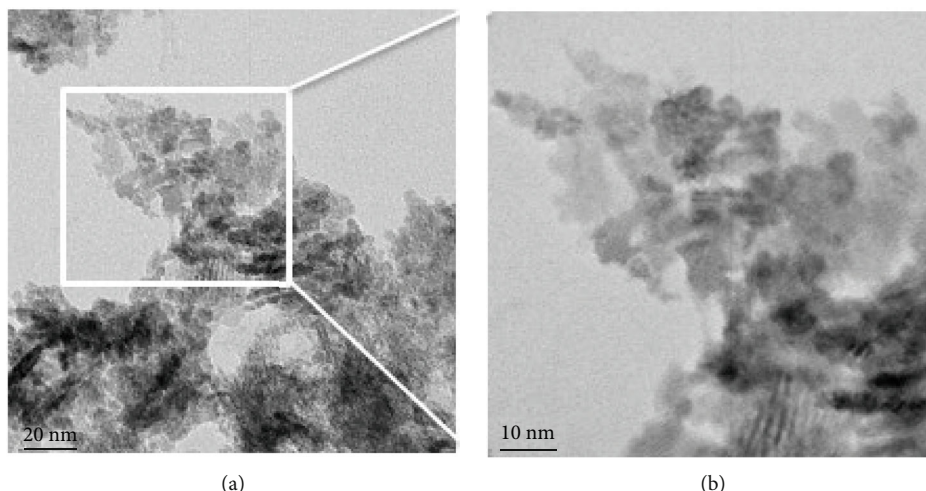


FIGURE 3: TEM images of PMMA with 0.7 wt. % MWCNT bone cement. (a) 20 nm scale and (b) 10 nm scale.

The heat dissipated during polymerization must be reduced to avoid thermal damage to the surrounding cells during *in situ* application. Berman et al. [21] reported that decreasing the operative temperature of PMMA-BC below 70°C might avoid severe bone necrosis at the bone and cement interface. Here, the percentage of damage to the bone cells is calculated as a damage function $D(T)$, which is defined as the time required to cause bone cell necrosis [22]. For instance, bone cell necrotizes and damage reaches 100% when it receives 60°C for 410 seconds. The amount of damage per second is calculated using Equation (2).

$$D(T) = \frac{1}{410} \times 100. \quad (2)$$

The thermal damage for the control, 0.1, 0.3, 0.5, and 0.7 wt. % MWCNT-loaded composite is noted as 0.73%, 0.64%, 0.61%, 0.63%, and 0.65%, respectively. It is observed that among the composites, thermal damage is minimal for 0.3 wt.% and maximum for 0.7 wt. % MWCNT loading. The heat dissipation duration is observed to influence thermal damage minimization. From this, it is evident that the curing kinetics of the PMMA-BC is affected by the inclusion of MWCNTs. The curing kinetics involves the setting time and duration of the polymerization reaction [23]. The increase in setting time provides additional time for processing/working during bone cement mixing. PMMA cement with varying amounts of MWCNTs and their respective setting times are summarized in Table 3. The initial and final setting times for PMMA-BC are found to be 605 ± 12 and 612 ± 15 seconds, respectively. The percentage increase in setting time for the prepared samples compared with PMMA-BC is found to be 0.65%, 1.15%, 2.30%, and 2.95% for BC1, BC2, BC3, and BC4, respectively.

The uniformly dispersed -COOH-functionalized MWCNTs are primarily responsible for the slow polymerization reaction (setting time) by physically impeding cross-linking of the polymer chains. The chemical functionalization of MWCNTs is found to improve the chemical interphase,

TABLE 3: Percentage variation in setting time and contact angle.

Bone cement samples	Setting time % \uparrow		Contact angle % \downarrow
	Initial	Final	
BC1	0.82 \uparrow	0.49 \uparrow	1.25 \downarrow
BC2	1.32 \uparrow	0.98 \uparrow	2.95 \downarrow
BC3	2.47 \uparrow	2.12 \uparrow	5.85 \downarrow
BC4	2.97 \uparrow	2.94 \uparrow	7.45 \downarrow

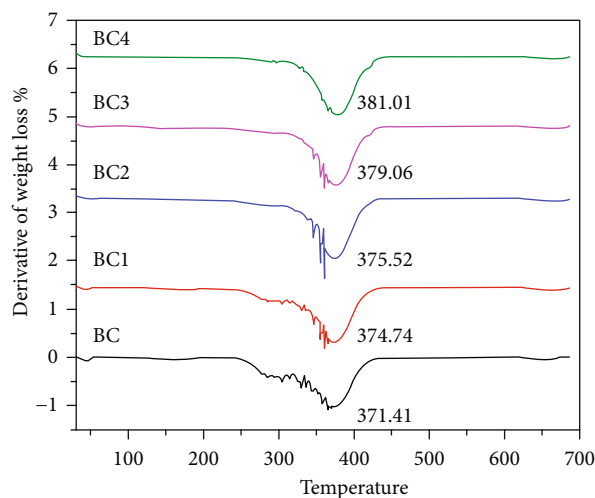


FIGURE 4: Derivative of TGA curves of composite bone cement.

and it is found to be the most predominant factor for a reduction in the peak polymerization temperature [24].

The derivative thermogravimetric analysis (DTG) of PMMA/MWCNTs composites is illustrated in Figure 4. The DTG plot revealed that the addition of MWCNTs delayed the thermal degradation of PMMA and increased its thermal stability. The degradation temperature of PMMA was determined as 371.41°C, which is increased by 0.89%,

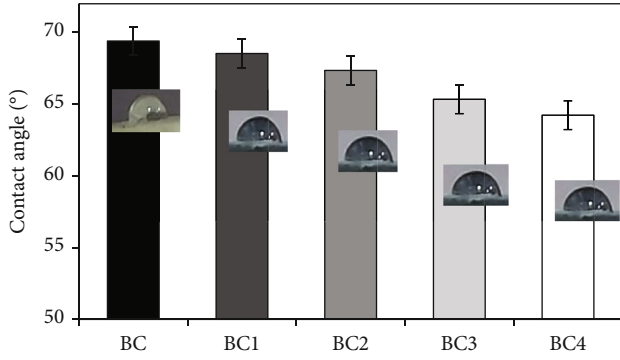


FIGURE 5: Contact angle of water droplets on composite bone cement.

1.1%, 2.1%, and 2.58% for 0.1, 0.3, 0.5, and 0.7 wt. % MWCNTs, respectively. This increase in thermal stability prevents the breakdown of PMMA beads of thickness 4–10 mm due to heat stresses when they are placed in the gap between the implant and bone [25].

6. Contact Angle

The contact angles for the distilled water droplets measured on the cement surface are presented in Figure 5. Water droplet photos revealed that the PMMA and PMMA/MWCNT composite bone cement surfaces are hydrophilic. However, nanocomposite bone cement samples have demonstrated a substantially lesser contact angle compared to PMMA-BC ($p < 0.04$). The contact angle for PMMA-BC is found as 69.40° . The percentage decrease in the contact angle for the composite bone cement samples is 1.25%, 2.95%, 5.85%, and 7.45% for BC1, BC2, BC3, and BC4, respectively. The contact angle is used to determine the surface energy (S_E) of the composite bone cement using Equation (3).

$$S_E = S_{EWA} \cos \theta \frac{J}{m^2}, \quad (3)$$

where S_{EWA} represents the surface energy between pure water and air at ambient temperature and pressure (72.8 mJ/m^2 at 20°C) [19] and " θ " represents the static contact angle. The percentage increase in surface energy for composite bone cement samples is found to be 4.03%, 9.45%, 18.59%, and 23.58% for BC1, BC2, BC3, and BC4, respectively.

Thus, it can be observed from the results of contact angle and surface energy that the reinforcement of -COOH-functionalized MWCNTs increased the wettability by decreasing hydrophobicity. Further, this facilitated the liquid monomer to wet the nanofillers effectively and improves the surface adhesion of the composite bone cement. The increase in surface wettability can also be verified by comparing it to the *in vitro* bioactivity studies. This improved surface wettability is found to increase mineral absorption and cell adhesion in simulated body fluid solution [19].

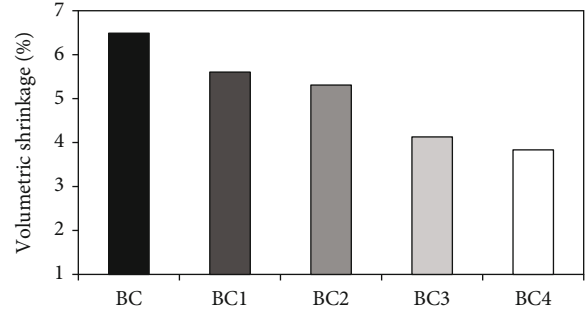


FIGURE 6: Volumetric shrinkage of composite bone cement.

TABLE 4: Volumetric shrinkage of the bone cement composition.

Material	% increase in density	% increase in the final volume	% reduction in volumetric shrinkage
BC1	4.06	0.94	13.63
BC2	4.40	1.26	18.18
BC3	6.10	2.52	36.36
BC4	7.03	2.83	40.90

7. Volumetric Shrinkage

The volume contraction of the prepared bone cement samples after curing is shown in Figure 6 as a volumetric shrinkage percentage. The initial volume (v_i) is calculated from the mould dimensions ($v_i = 0.339 \text{ mL}$), and Archimedes' principle is used to measure the final volume (v_f) by measuring density. The volumetric shrinkage for PMMA-BC is found to be 6.49% after curing, whereas for nanocomposite bone cement it is observed to be 5.60%, 5.31%, 4.13%, and 3.83% for BC1, BC2, BC3, and BC4, respectively.

Table 4 summarizes the density variations, dimensional changes, and reduction in shrinkage for the cured nanocomposite samples. The volume shrinkage of PMMA/MWCNT composite bone cement is observed to be 13.63%, 18.18%, 36.36%, and 40.90% for BC1, BC2, BC3, and BC4, respectively, compared with PMMA-BC. The maximum reduction in volumetric shrinkage occurred in BC4, which indicates that the volumetric shrinkage is directly proportional to the MWCNT concentration.

Volumetric shrinkage is an extrinsic property inversely proportional to the density of the polymer (Equation (1)). The density of MMA was specified by the manufacturer as 0.938–0.940 g/cc before curing. However, the density of PMMA-BC is noted as 1.18 g/cc after curing. The density of the composite bone cement is increased with the reinforcement of MWCNTs [26]. This increased density is the consequence of the reduction in the number of cross-connections between MWCNTs and the PMMA matrix [27]. The rise in density is observed to increase the molecular weight, and it leads to a reduction in volumetric shrinkage [28]. It is observed that the polymerization shrinkage is extensive in the viscous phase of the cement curing. The volumetric shrinkage may be attributed to polymerization

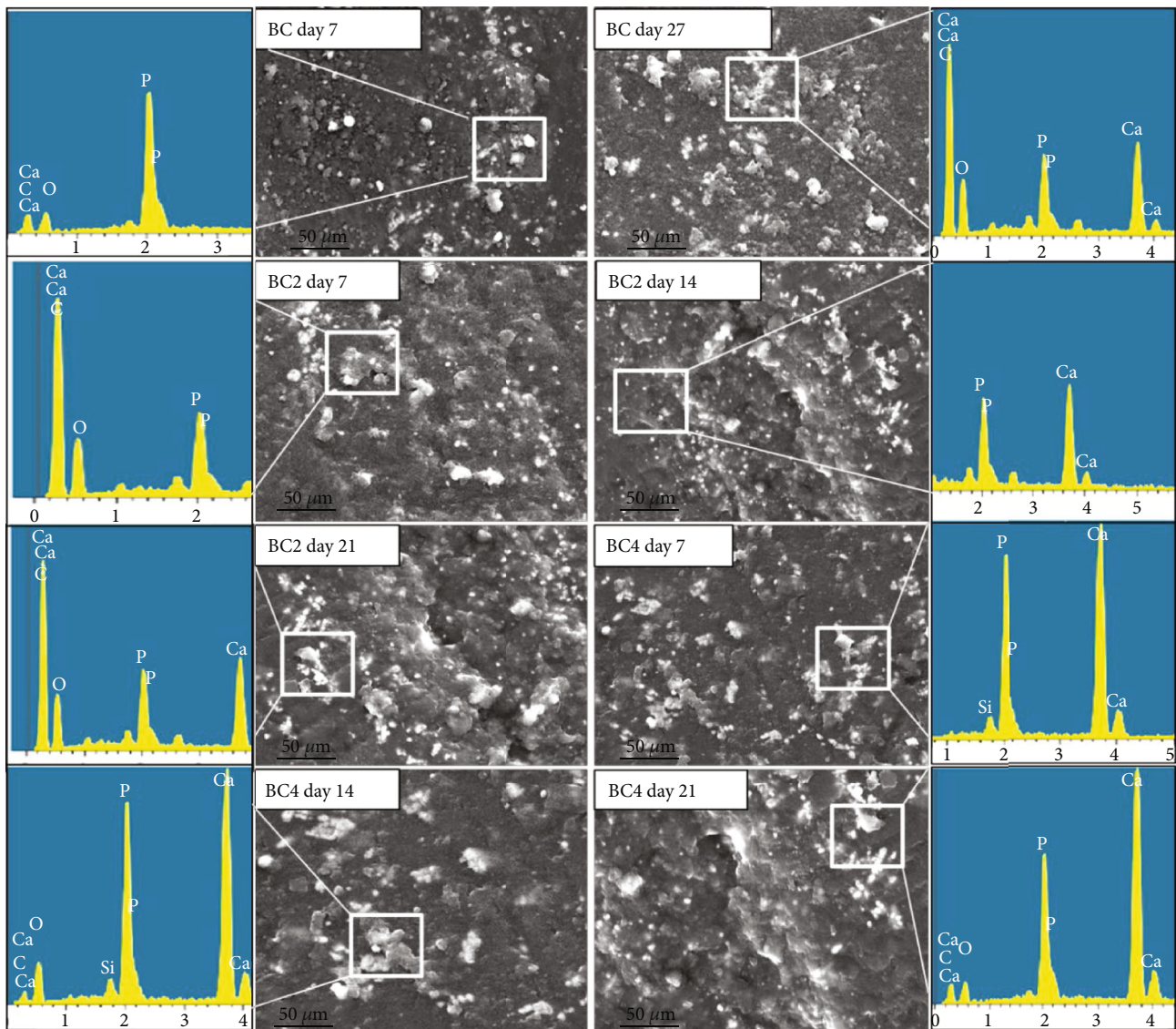


FIGURE 7: SEM pictures with boxed EDS spectra show bone cement biomimetalization in SBF.

shrinkage, thermal contraction after the exothermic reaction, and cement density [29]. Another important parameter responsible for volume shrinkage is the mixing method, and it is a fact that the bone cement shrinks in a confined environment forming pores at the cement implant interface anywhere during polymerization. In this study, the hand mixing method is used, during which some shrinkage occurred at the pore sites, which is notable in the volume reduction. Therefore, better mechanical properties can be expected at the cement-implant interface with lower volumetric shrinkage.

7.1. In Vitro Bioactivity. The nanocomposite bone cement sample disks containing 0.3 and 0.7 wt. % MWCNTs are subjected to *in vitro* bioactivity studies. Because of its intended application in bone tissue, bone cement requires bioactivity to ensure a reliable bonding of PMMA-BC right after the surgery. SEM images of the composite bone cement

sample after soaking in SBF for 7, 14, and 21 days (Figure 7) revealed that the nucleation of primary apatite has a nodular structure. The samples are subjected to EDS analysis on the selected area and the deposition of Ca and P elements are observed. The increased intensities of Ca and P peaks are observed on the sample surface, confirming the deposition of mineral phases through SEM-EDS spectra [21]. The increased deposition with grown individual nuclei and a reticular layer composed of secondary apatite (numerous flakes) due to coalescence are observed after 21 days. Despite certain deposits being visible on the surface of the sample, the EDS examination after 7 days of immersion revealed the absence of Ca or P elements.

FTIR is used to identify functional groups and characterize the chemical structures based on the interaction of infrared radiation with matter. The peaks observed in the transmission spectra are depicted in Figure 8. The peaks observed in the range of $1395\text{--}1440\text{ cm}^{-1}$ correspond to the

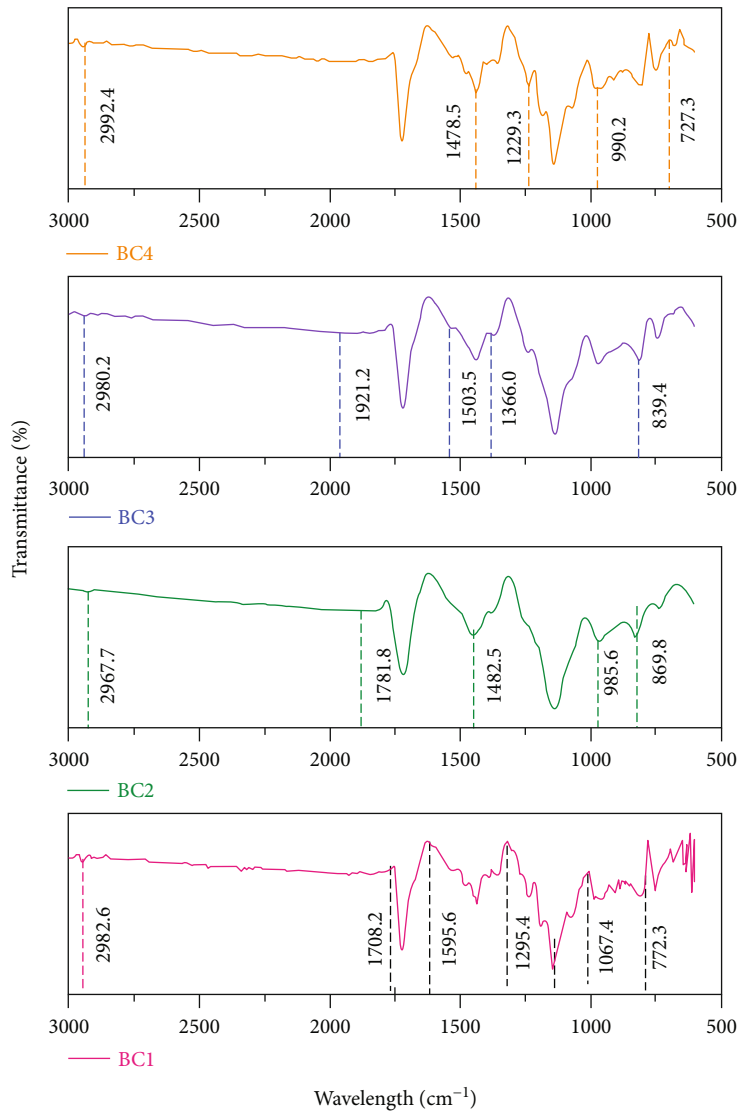


FIGURE 8: FTIR spectra of the PMMA composite bone cement.

O–H bond. The peaks observed from 815 to 930 cm^{-1} can be assessed to the valence C=O bond. The CC stretching vibration bands of MWCNT are found at the peaks of 1503 and 1482 cm^{-1} . The sharp peaks could be attributed to the existence of the -COOH functional groups. These results are observed to indicate the physical bonding between the MWCNT-COOH and PMMA matrix, which has influenced the nanocomposite for more wettability. Thus, the enhanced bioactivity is observed after 21 days of immersion, and it is mainly due to the incorporation of -COOH-functionalized MWCNTs.

8. Discussion

In this study, it is shown that adding a small amount of carboxyl functionalized MWCNT enhanced the bioactivity and cement characteristics of proprietary Simplex P bone cement. The decrease in polymerization temperature, reduction in volumetric shrinkage, and increased surface wettabil-

ity are observed after MWCNT-COOH incorporation. The homogeneous distribution of MWCNT within the PMMA-BC matrix is considered an important parameter for the enhancements in cement properties [30]. It is possible that the -COOH groups attached to the MWCNTs, which are negatively charged, contributed to the uniform dispersion [31]. The existence of uniformly dispersed MWCNT-COOH inside the PMMA-BC matrix leads to a decrease in agglomerations. Agglomerations can further contribute as a site for the stress concentration, leading to crack initiation and early fracture of the cement mantle [16, 32]. Subsequently, the uniform dispersion would also expedite a higher amount of chemical interaction between the MWCNT-COOH and the PMMA-BC matrix, resulting in effective stress transfer. Therefore, the evenly distributed MWCNTs in the novel nanocomposite bone cement could be able to prolong the functionality of the existing PMMA-BC.

This study found the reduction in Simplex P bone cement's exothermic polymerization reaction, which would

reduce thermal shrinkage-induced residual stresses [33]. Incorporating a 0.1–0.7 wt. % of MWCNT-COOH helped to dissipate heat from the nanocomposite bone cement's exothermic polymerization reaction. Interestingly, the MWCNT-COOH used in this study has a thermal conductivity of more than 3000 W/mK (Platonic data sheet), indicating that it acted as a heat sink in the nanocomposite to dissipate the heat produced during polymerization. The addition of 0.3 wt. % MWCNT reduced the thermal damage $D(T)$ per second by 16% (maximum) compared with PMMA bone cement. Ormsby et al. [30] also reported that the incorporation of MWCNTs into acrylic bone cement has reduced the peak polymerization temperature by 34% and the thermal necrosis index values are significantly reduced at $\geq 44^\circ\text{C}$ and $\geq 55^\circ\text{C}$ (28% and 27%) compared to PMMA bone cement. In this study, it can be noted that the thermal damage is minimum at 0.3 wt. %, and it is also lesser than the thermal necrosis index values which were observed from the published work. The slower rate of polymerization and lower T_{max} decreased the exposure time of bone tissue to high temperatures. This helps to reduce the damage function $D(T)$ and provides adequate workability in preparing and placing the cement mantle. The DSC analysis carried out in this study revealed an increase in thermal stability, which would also support this observation.

The workability of any bone cement depends on its initial and final setting time. Shaping and filling of bone cement are required enough initial setting time. Disturbing the prepared cement until it hardens will cause fractures and weaken it. It needs the shortest final setting time to avoid wound closure delays. The initial setting time shows the end of the workability of cement after wetness, whereas the final setting time signifies the cement hardening. Ormsby et al. [16] observed a 3–24% increase in setting time when 0.1 wt. % of MWCNTs incorporated into PMMA-BC. However, these variations were observed for different methods of incorporation and functionalized/nonfunctionalized groups. In this study, the setting times for the prepared composite bone cement samples are well within the admissible setting time for orthopedic applications [34].

Bone cement shrinkage is another aspect hypothesized to contribute to implant loosening. In this study, the volumetric shrinkage for PMMA-BC is found to be 6.49% after curing, whereas for BC1, BC2, BC3, and BC4, it is observed to be 5.60%, 5.31%, 4.13%, and 3.83%, respectively. Gilbert et al. [9] also reported that volumetric shrinkage for Simplex P bone cement as a result of density variation, due to the exothermic polymerization, was between 5.1% and 6.5%, depending on the mixing method employed and the type of cement. Jasty et al. [35] discovered cracks emanating from the inner surface of the cement mantle and indicated that they were caused by hoop stresses due to acrylic cement shrinkage during polymerization. Hence, the reduction in volumetric shrinkage observed in this study is better compared to the previous results and helps in avoiding cracks by reducing the hoop stresses.

The wettability of the cement helps in the adsorption of more proteins and minerals leading to enhance binding sites for cell attachment on the cement surface. In this study, the

wettability is calculated using the contact angle of bone cement with distilled water droplets. The addition of MWCNTs decreased the contact angle and increased the wettability. The surface energy of PMMA-BC is increased to 31.64 mJ/m² by the addition of 0.7 wt. % MWCNT-COOH, whereas for the PMMA bone cement, it is observed to be 25.60 mJ/m². Jayasree and Sampath Kumar [19] also studied the effect of wettability in improving the bioactivity of commercially available orthopedic bone cement, where the surface energy of Simplex P bone cement is measured to be 25.67 mJ/m² with the addition of 25 wt. % calcium-deficient hydroxyapatite.

The current research has a few limitations that are acknowledged. Firstly, just one type of cement (Simplex P) was employed because other varieties with various chemical compositions and viscosities could produce different results. Since total hip and knee replacements is using Simplex P as one of the most popular bone cement formulations, this particular cement was chosen [36]. Secondly, the mechanical properties of the MWCNT-loaded cement were not evaluated, although they play a significant role in *in vivo* cement failure. Mechanical characterization is found to be out of the scope of the current investigation. Thirdly, only *in vitro* bioactivity tests were carried out, but antimicrobial studies would have revealed distinct effects. However, *in vitro* testing greatly simplifies the *in vivo* situation, and care must be given when interpreting biocompatibility data.

9. Conclusion

The results of earlier research have been expanded in this study to improve the cement properties and thermal characteristics of commercially available Simplex P bone cement by incorporating MWCNT-COOH using the geometric dilution method. The influence of 0.1, 0.3, 0.5, and 0.7 wt. % MWCNTs on cement properties and *in vitro* bioactivity studies of the polymerizing and cured cement are examined. The uniform distribution of MWCNT-COOH was assumed to reduce the exothermic polymerization reaction. Here, the maximum reduction in the peak polymerization temperature of 29% is found in the BC4 samples. This reduction in T_{max} is influencing the setting time of the samples, and for BC4, the setting time is prolonged by 2.94%. The increase in surface wettability (23.58%↑) and setting time (2.94%↑) and decrease in maximum polymerization temperature (29.06%↓) and volumetric shrinkage (40.9%↓) are observed for MWCNT-loaded composite bone cement relative to the control cement (without MWCNTs). The *in vitro* bioactivity test results indicate that the mineral deposition is observed to be proportional with MWCNTs wt.% which is increased wettability of the cement. These findings imply that *in vitro* and *in vivo* biocompatibility studies of -COOH-functionalized MWCNT-loaded with PMMA-BC may be tested for their feasibility to understand the clinical usage complications.

Data Availability

The data used to support the results of this study are included in the article.

Conflicts of Interest

The authors declare that they have no known competing financial interests or personal connections that could have influenced the findings of this study.

Acknowledgments

The authors are thankful to the Siddaganga Institute of Technology, Tumakuru, for providing a research facility, the Visvesvaraya Technological University, Belagavi, Karnataka, India, for supporting this research work, and the Biotechnology Department, Siddaganga Institute of Technology, Tumakuru, and the BioEdge Solutions, Peenya, Bengaluru 560058, for supporting in conducting biocompatibility studies. The authors appreciate the support from the Seenu Atoll School, Maldives, for the preparation of the manuscript. The authors thank the generous support from the Department of Applied Sciences (Nanotechnology), Visvesvaraya Technological University, Center for Post Graduate Studies, Bengaluru Region, Muddenahalli, Chikkballapura 562101, Karnataka, India, for supporting the characterizations. The authors thank the Vision Group on Science and Technology, Department of Electronics, Information Technology, Biotechnology and Science & Technology, Government of Karnataka, the Advanced Composites Division, CSIR-National Aerospace Laboratories, Bengaluru 560017, Karnataka, India, and the Center of Applied Research and Nanotechnology, Siddaganga Institute of Technology, Tumakuru, for conducting this research work.

References

- [1] L. Hasandoost, O. Rodriguez, A. Alhalawani et al., "The role of poly(methyl methacrylate) in management of bone loss and infection in revision total knee arthroplasty: A Review," *Journal of Functional Biomaterials*, vol. 11, no. 2, p. 25, 2020.
- [2] M. E. Zapata, C. D. Tovar, and J. H. Hernandez, "The role of chitosan and graphene oxide in bioactive and antibacterial properties of acrylic bone cements," *Biomolecules*, vol. 10, no. 12, p. 1616, 2020.
- [3] D. O. Ko, S. Lee, K. T. Kim, J. Il Lee, J. W. Kim, and S. M. Yi, "Cement mantle thickness at the bone cement interface in total knee arthroplasty: comparison of PS150 RP and LPS-flex knee implants," *Knee Surgery & Related Research*, vol. 29, no. 2, pp. 115–121, 2017.
- [4] A. Rajan, V. Thirunarayanan, D. R. Ramprasath, J. D. V. Kumar, and K. Muthulingam, "Vertebroplasty in osteoporotic vertebral fractures: technical considerations and complications," *Journal of Orthopedics and Joint Surgery*, vol. 2, no. 1, pp. 17–21, 2020.
- [5] N. Dunne, J. Clements, and J.-S. Wang, "Acrylic cements for bone fixation in joint replacement," in *Joint Replacement Technology*, pp. 212–256, Elsevier, 2014.
- [6] P. A. Revell, "Biological causes of prosthetic joint failure," in *Joint Replacement Technology*, pp. 299–371, Elsevier, 2021.
- [7] R. Vaishya, M. Chauhan, and A. Vaish, "Bone cement," *Journal of Clinical Orthopaedics and Trauma*, vol. 4, no. 4, pp. 157–163, 2013.
- [8] N. Dunne and W. Ross, "MWCNT used in orthopaedic bone cements," in *Carbon Nanotubes - Growth and Applications*, IntechOpen, 2011.
- [9] J. L. Gilbert, J. M. Hasenwinkel, R. L. Wixson, and E. P. Lautenschlager, "A theoretical and experimental analysis of polymerization shrinkage of bone cement: a potential major source of porosity," *Journal of Biomedical Materials Research*, vol. 52, no. 1, pp. 210–218, 2000.
- [10] A. De Mori, E. Di Gregorio, A. P. Kao et al., "Antibacterial PMMA composite cements with tunable thermal and mechanical properties," *ACS Omega*, vol. 4, no. 22, pp. 19664–19675, 2019.
- [11] J. Slane, J. Vivanco, W. Rose, H.-L. Ploeg, and M. Squire, "Mechanical, material, and antimicrobial properties of acrylic bone cement impregnated with silver nanoparticles," *Materials Science and Engineering: C*, vol. 48, pp. 188–196, 2015.
- [12] K. Letchmanan, S. C. Shen, W. K. Ng et al., "Mechanical properties and antibiotic release characteristics of poly(methyl methacrylate)-based bone cement formulated with mesoporous silica nanoparticles," *Journal of the Mechanical Behavior of Biomedical Materials*, vol. 72, pp. 163–170, 2017.
- [13] F. Pahlevanzadeh, H. R. Bakhsheshi-Rad, A. F. Ismail, M. Aziz, and X. B. Chen, "Development of PMMA-Mon-CNT bone cement with superior mechanical properties and favorable biological properties for use in bone-defect treatment," *Materials Letters*, vol. 240, pp. 9–12, 2019.
- [14] N. Baig, I. Kammakakam, and W. Falath, "Nanomaterials: a review of synthesis methods, properties, recent progress, and challenges," *Materials Advances*, vol. 2, no. 6, pp. 1821–1871, 2021.
- [15] S. Soleymani Eil Bakhtiari, H. R. Bakhsheshi-Rad, S. Karbasi et al., "Polymethyl methacrylate-based bone cements containing carbon nanotubes and graphene oxide: an overview of physical, mechanical, and biological properties," *Polymers*, vol. 12, no. 7, p. 1469, 2020.
- [16] R. Ormsby, T. McNally, C. Mitchell, and N. Dunne, "Incorporation of multiwalled carbon nanotubes to acrylic based bone cements: effects on mechanical and thermal properties," *Journal of the Mechanical Behavior of Biomedical Materials*, vol. 3, no. 2, 2010.
- [17] K. D. Patel, R. K. Singh, and H.-W. Kim, "Carbon-based nanomaterials as an emerging platform for theranostics," *Materials Horizons*, vol. 6, no. 3, pp. 434–469, 2019.
- [18] S. Tantavisut, J. Leanpolchareanchai, and A. Wongrakpanich, "Influence of chitosan and chitosan oligosaccharide on dual antibiotic-loaded bone cement: in vitro evaluations," *PLoS One*, vol. 17, no. 11, article e0276604, 2022.
- [19] R. Jayasree and T. Sampath Kumar, "Acrylic cement formulations modified with calcium deficient apatite nanoparticles for orthopaedic applications," *Journal of Composite Materials*, vol. 49, no. 23, pp. 2921–2933, 2015.
- [20] G. Lewis, "Properties of nanofiller-loaded poly (methyl methacrylate) bone cement composites for orthopedic applications: a review," *Journal of Biomedical Materials Research Part B: Applied Biomaterials*, vol. 105, no. 5, pp. 1260–1284, 2017.
- [21] A. T. Berman, J. S. Reid, D. R. Yanicko, G. C. Sih, and M. R. Zimmerman, "Thermally induced bone necrosis in rabbits," *Clinical Orthopaedics and Related Research*, vol. 186, pp. 284–292, 1984.
- [22] H. Fukushima, Y. Hashimoto, S. Yoshiya et al., "Conduction analysis of cement interface temperature in total knee

- arthroplasty,” *Kobe Journal of Medical Sciences*, vol. 48, no. 1–2, pp. 63–72, 2002.
- [23] R. Ormsby, T. McNally, C. Mitchell, and N. Dunne, “Influence of multiwall carbon nanotube functionality and loading on mechanical properties of PMMA/MWCNT bone cements,” *Journal of Materials Science. Materials in Medicine*, vol. 21, no. 8, pp. 2287–2292, 2010.
- [24] R. Ormsby, T. McNally, C. Mitchell et al., “Effect of MWCNT addition on the thermal and rheological properties of polymethyl methacrylate bone cement,” *Carbon*, vol. 49, no. 9, pp. 2893–2904, 2011.
- [25] S. K. Smart, A. I. Cassady, G. Q. Lu, and D. J. Martin, “The biocompatibility of carbon nanotubes,” *Carbon*, vol. 44, no. 6, pp. 1034–1047, 2006.
- [26] B. Pei, W. Wang, N. Dunne, and X. Li, “Applications of carbon nanotubes in bone tissue regeneration and engineering: superiority, concerns, current advancements, and prospects,” *Nanomaterials*, vol. 9, no. 10, p. 1501, 2019.
- [27] H. Kim, B. Goh, S. Lee, K. Lee, and J. Choi, “Computational study on interfacial interactions between polymethyl methacrylate-based bone cement and hydroxyapatite in nanoscale,” *Applied Sciences*, vol. 11, no. 7, p. 2937, 2021.
- [28] N. Dunne, A. Tzagiollari, M. Sahebalzamani, and T. J. Dunne, “Acrylic cements for bone fixation in joint replacement,” in *Joint Replacement Technology*, pp. 213–262, Elsevier, 2021.
- [29] A. Alnazzawi and D. C. Watts, “Simultaneous determination of polymerization shrinkage, exotherm and thermal expansion coefficient for dental resin-composites,” *Dental Materials*, vol. 28, no. 12, pp. 1240–1249, 2012.
- [30] R. W. Ormsby, M. Modreanu, C. A. Mitchell, and N. J. Dunne, “Carboxyl functionalised MWCNT/polymethyl methacrylate bone cement for orthopaedic applications,” *Journal of Biomaterials Applications*, vol. 29, no. 2, pp. 209–221, 2014.
- [31] M. Chao, Y. Li, G. Wu, Z. Zhou, and L. Yan, “Functionalized multiwalled carbon nanotube-reinforced polyimide composite films with enhanced mechanical and thermal properties,” *International Journal of Polymer Science*, vol. 2019, Article ID 9302803, 12 pages, 2019.
- [32] B. Marrs, R. Andrews, T. Rantell, and D. Pienkowski, “Augmentation of acrylic bone cement with multiwall carbon nanotubes,” *Journal of Biomedical Materials Research Part A*, vol. 77A, no. 2, pp. 269–276, 2006.
- [33] N. J. Dunne and J. F. Orr, “Curing characteristics of acrylic bone cement,” *Journal of Materials Science. Materials in Medicine*, vol. 13, no. 1, pp. 17–22, 2002.
- [34] E. Şahin, “Calcium phosphate bone cements,” in *Cement Based Materials*, INTECH, 2018.
- [35] M. Jasty, W. Maloney, C. Bragdon, D. O’Connor, T. Haire, and W. Harris, “The initiation of failure in cemented femoral components of hip arthroplasties,” *Journal of Bone and Joint Surgery (British Volume)*, vol. 73-B, no. 4, pp. 551–558, 1991.
- [36] S. Kim, A. R. Bishop, M. W. Squire, W. E. Rose, and H.-L. Ploeg, “Mechanical, elution, and antibacterial properties of simplex bone cement loaded with vancomycin,” *Journal of the Mechanical Behavior of Biomedical Materials*, vol. 103, article 103588, 2020.